Received: 5 January 2024 | Revised: 28 February 2024 | Accepted: 3 March 2024

DOI: 10.1111/pce.14884

ORIGINAL ARTICLE

Plant, Cell & Environment | WILEY

The development of pleiotropic phenotypes in powdery mildew-resistant barley and *Arabidopsis thaliana mlo* mutants is linked to nitrogen availability

Matthias Freh[1] | Anja Reinstädler[1] | Kira D. Neumann[1] | Ulla Neumann[2] | Ralph Panstruga[1]

[1]Unit of Plant Molecular Cell Biology, Institute for Biology I, RWTH Aachen University, Aachen, Germany

[2]Central Microscopy, Max Planck Institute for Plant Breeding Research, Cologne, Germany

Correspondence
Ralph Panstruga, Unit of Plant Molecular Cell Biology, Institute for Biology I, RWTH Aachen University, Worringerweg 1, 52056 Aachen, Germany.
Email: panstruga@bio1.rwth-aachen.de

Funding information
Novo Nordisk Foundation, Grant/Award Number: NNF19OC0056457

Abstract

Powdery mildew-resistant barley (*Hordeum vulgare*) and *Arabidopsis thaliana mlo* mutant plants exhibit pleiotropic phenotypes such as the spontaneous formation of callose-rich cell wall appositions and early leaf chlorosis and necrosis, indicative of premature leaf senescence. The exogenous factors governing the occurrence of these undesired side effects remain poorly understood. Here, we characterised the formation of these symptoms in detail. Ultrastructural analysis revealed that the callose-rich cell wall depositions spontaneously formed in *A. thaliana mlo* mutants are indistinguishable from those induced by the bacterial pattern epitope, flagellin 22 (flg22). We further found that increased plant densities during culturing enhance the extent of the leaf senescence syndrome in *A. thaliana mlo* mutants. Application of a liquid fertiliser rescued the occurrence of leaf chlorosis and necrosis in both *A. thaliana* and barley *mlo* mutant plants. Controlled fertilisation experiments uncovered nitrogen as the macronutrient whose deficiency promotes the extent of pleiotropic phenotypes in *A. thaliana mlo* mutants. Light intensity and temperature had a modulatory impact on the incidence of leaf necrosis in the case of barley *mlo* mutant plants. Collectively, our data indicate that the development of pleiotropic phenotypes associated with *mlo* mutants is governed by various exogenous factors.

KEYWORDS
Barley, callose deposits, leaf chlorosis, leaf necrosis, *mlo* resistance

1 | INTRODUCTION

Plant *MLO* genes encode integral membrane proteins that were recently found to operate as cation channels (Gao et al., 2022, 2023). The founder of the gene family, barley *Mlo*, was originally identified as a susceptibility factor in the context of infection with the fungal powdery mildew pathogen *Blumeria hordei* (formerly designated as *Blumeria graminis* f.sp. *hordei*; Liu, Braun, et al., 2021). Accordingly, recessively inherited loss-of-function mutations in barley *Mlo* confer durable broad-spectrum resistance against the disease (Büschges et al., 1997; Jørgensen, 1992). Subsequently it was discovered that *Mlo* genes are present in all photosynthetically active eukaryotes. In

Abbreviations: BSA, bovine serum albumin; flg22, 22-amino acid elicitor epitope of bacterial flagellin; Mlo, mildew resistance locus o; SA, salicylic acid.

land plant species, they occur as medium-sized gene families comprising approximately 10–40 members (Kusch et al., 2016). Accordingly, *mlo*-based resistance can be found in a wide variety of plant species (Kusch & Panstruga, 2017). Mlo/MLO proteins (note that the nomenclature differs by species) of particular phylogenetic clades seem to be associated with specific physiological processes (Acevedo-Garcia, Gruner, et al., 2017; Kusch et al., 2016). For example, the capacity to serve as a susceptibility factor to powdery mildew disease is associated with members of phylogenetic clades IV and V (Kusch et al., 2016). In the dicotyledonous reference plant *Arabidopsis thaliana*, three *MLO* genes (*MLO2*, *MLO6*, and *MLO12*) contribute unequally to this phenotype: While *mlo2* mutants exhibit partial resistance to powdery mildew disease, *mlo2 mlo6 mlo12* triple mutants are fully resistant (Acevedo-Garcia, Gruner, et al., 2017; Consonni et al., 2006).

Apart from conferring broad-spectrum powdery mildew resistance, barley *mlo* and *A. thaliana mlo2* single mutants, *mlo2 mlo6* and *mlo2 mlo12* double mutants, as well as *mlo2 mlo6 mlo12* triple mutants suffer from pleiotropic phenotypes. These are macroscopically visible as premature leaf chlorosis and necrosis, which are preceded by the spontaneous and seemingly erratic deposition of callose-containing cell wall appositions in leaf mesophyll cells, which earlier have been interpreted as signs of uncontrolled defence (Consonni et al., 2006; Schwarzbach, 1976; Wolter et al., 1993). In the case of barley *mlo* mutants, it was shown that this syndrome is not pathogen-dependent and even developed by plants grown in sterile conditions (Wolter et al., 1993). It is associated with a premature decay of photosynthesis pigments (Consonni et al., 2010; Piffanelli et al., 2002), an accelerated decline in photosynthetic performance (Consonni et al., 2010), a modified transcriptional programme (Consonni et al., 2010), and altered levels of defence-associated indolic secondary metabolites (Consonni et al., 2010), ultimately cumulating in spontaneous leaf mesophyll cell death (Peterhansel et al., 1997) in the course of plant development. Altogether, it has been interpreted as either representing a lesion-mimic phenotype, mirroring an uncontrolled plant defence response (Wolter et al., 1993), or reflecting an untimely senescence programme (Consonni et al., 2010; Piffanelli et al., 2002).

The undesirable side effects initially hampered the usefulness of barley *mlo* mutants in agriculture as they were found to be associated with a marked yield penalty (Jørgensen, 1992; Schwarzbach, 1976). It turned out, however, that the extent of the pleiotropic phenotypes relies on the particular *mlo* allele and the genetic background of the respective mutant: Partial loss-of-function barley *mlo* mutants, conferring incomplete powdery mildew resistance, exhibit less severe leaf chlorosis and necrosis than *mlo* null mutants (Ge et al., 2016, 2020; Habekuss & Hentrich, 1988; Hentrich & Habekuss, 1993; Hentrich, 1979). In addition, even in the case of the same *mlo* allele, the genetic background modulates the extent of the associated pleiotropic phenotypes (Bjørnstad & Aastveit, 1990). Especially the latter aspect led to the breeding of *mlo*-resistant barley elite cultivars, which are free of untimely leaf decay and that are nowadays widely used in European agriculture (Dreiseitl, 2022; Lyngkjær et al., 2000).

Genetic analysis in *A. thaliana* revealed that the development of leaf chlorosis/necrosis and the occurrence of callose-rich cell wall appositions in *mlo2* mutants depends on the phytohormone salicylic acid (SA). In *mlo2* single and *mlo2 mlo6 mlo12* triple mutants, SA hyperaccumulates during development, resulting in strongly increased levels of free and conjugated SA in the rosette leaves of 6- and 7-week-old plants (Consonni et al., 2006; Lorek et al., 2013). Double mutants defective in *MLO2* and components of SA biosynthesis (*SALICYLIC ACID INDUCTION DEFICIENT 2*, *SID2*), transport (*ENHANCED DISEASE SUSCEPTIBILITY 5*, *EDS5*) or signalling (*NONEXPRESSER OF PR GENES 1*, *NPR1*; *PHYTOALEXIN DEFICIENT 4*, *PAD4*), or *mlo2* mutants transgenically depleted of SA (*NahG* overexpression) show a rescue of the pleiotropic phenotypes yet retain full powdery mildew resistance (Consonni et al., 2006). Genetic epistasis analysis further revealed that POWDERY MILDEW RESISTANT 4 (PMR4) is the callose synthase responsible for the biosynthesis of the β-1,3-glucan polymer present in *mlo2*-conditioned cell wall appositions (Consonni et al., 2010). In addition, the heterotrimeric G-protein γ subunit AGG1 (Lorek et al., 2013) as well as the transcriptional modulator RADICAL-INDUCED CELL DEATH 1 (RCD1; (Cui et al., 2018)) further control the occurrence of the callose-rich depositions. The perturbed accumulation of indolic secondary metabolites also seen in *A. thaliana mlo2* mutants can be genetically separated from leaf chlorosis/necrosis, as double mutants defective in *mlo2* and the biosynthesis of these compounds retain this phenotype (Consonni et al., 2010). In case of a hexaploid wheat *mlo* mutant, the ectopic activation of the B genome-associated *Tonoplast monosaccharide transporter 3* (*TMT3B*) was recently found to uncouple powdery mildew resistance from growth and yield penalties that are otherwise associated with this mutant (Li et al., 2022).

Although, in principle, the manifestation of developmentally controlled pleiotropic phenotypes in powdery mildew-resistant barley and *A. thaliana mlo* mutants is robust and highly reproducible, their extent and timing can be variable (Consonni et al., 2006). It seems as if hitherto unrecognised parameters modulate their appearance and severity. To explore the nature of these yet unknown factors, we here performed a comprehensive phenotypic characterisation of the pleiotropic phenotypes in barley *mlo* and *A. thaliana mlo2* (*mlo6 mlo12*) single/triple mutants. We used transmission electron microscopy to study the ultrastructure of *mlo2*-induced callose depositions, revealed plant crowding as a factor exaggerating the pleiotropic phenotypes, and identified fertilisation, in particular the supply of nitrogen, as a treatment reverting the enhancing effect of plant crowding. We further recognised soil type as a key component of phenotype severity and investigated the effect of temperature and light intensity on the formation of leaf necrotic spots in a barley *mlo* genotype. In summary, our study reveals features that modulate the occurrence and extent of the developmentally controlled pleiotropic phenotypes of *A. thaliana* and barley *mlo* mutants.

2 | RESULTS

2.1 | Ultrastructural analysis of spontaneous callose depositions in *A. thaliana mlo2 mlo6 mlo12* mutant plants

The *mlo*-associated spontaneous callose depositions have been previously interpreted as putative signs of an uncontrolled defence response ("defence/lesion mimic phenotype"; Martienssen, 1997; Wolter et al., 1993). However, whether the callose-rich cell wall appositions formed in the context of authentic plant immunity and *mlo*-induced callose deposits are indeed similar at the ultrastructural level remained elusive. Such resemblance could lend additional support for the hypothesis that these structures are formed by the same cellular pathway(s). We here exploited the capacity of the pathogen-derived molecular pattern epitope flg22, a 22-amino acid fragment of bacterial flagellin, to trigger a genuine immune response, and compared the induced cell wall appositions with those formed spontaneously in leaves of an *A. thaliana mlo* mutant by transmission electron microscopy (TEM). To this end, we grew ecotype Col-0 wild-type and *mlo2*-5 *mlo6*-2 *mlo12*-1 triple mutant plants to the age of 7 weeks, when *mlo* triple mutant plants usually exhibit spontaneous callose depositions (Consonni et al., 2006; Consonni et al., 2010). Rosette leaves were then treated with flg22 (Col-0), submitted to a respective mock treatment (Col-0), or left untreated (Col-0 and *mlo* triple mutant; see Materials and Methods for details). The next day, leaves were split longitudinally into two halves: While one half was subjected to histochemical Aniline blue staining and subsequent epifluorescence microscopy to validate the occurrence of callose depositions in the specimens (Supporting Information S1: Figure 1A–D), the other half was processed for subsequent immunodetection of callose by both light microscopy (Supporting Information S1: Figure 1E–H) and TEM (Supporting Information S1: Figure 1I–P).

Aniline blue staining revealed that in untreated and mock-treated leaves of Col-0 plants, fluorescence was mainly detectable as autofluorescence of trichomes on the leaf surface (Supporting Information S1: Figure 1A,B). By contrast, flg22-treated Col-0 leaves as well as untreated *mlo* triple mutant leaves showed numerous fluorescent spots distributed over the leaf laminae in addition to trichome-related autofluorescence (Supporting Information S1: Figure 1C,D). Immunofluorescence analysis of leaf cross sections of these sample types with a mouse monoclonal anti-β-1,3-glucan antibody, detected by a fluorophore-tagged secondary goat anti-mouse antibody, revealed extended regions of callose deposition along cell walls, primarily of leaf mesophyll cells but also of adaxial and abaxial epidermal cells, and especially at cell-cell junctions (Supporting Information S1: Figure 1E–H).

In sections of untreated and mock-treated Col-0 rosette leaves, immunogold labelling with the same mouse monoclonal anti-β-1,3-glucan antibody detected by a secondary goat anti-mouse antibody conjugated to 10 nm colloidal gold particles, epitope detection was essentially restricted to plasmodesmata and, occasionally, to the vacuolar lumen and newly deposited cell walls in the vascular cambium (Supporting Information S1: Figure 1I,J). By contrast, leaf sections of flg22-treated Col-0 (Supporting Information S1: Figure 1K,L) or untreated *mlo2 mlo6 mlo12* mutant leaves (Supporting Information S1: Figure 1M–P) frequently exhibited profuse gold labelling. Consistent with the results after Aniline blue staining (Supporting Information S1: Figure 1C,D) and immunofluorescence microscopy (Supporting Information S1: Figure 1E–H), in both cases, gold particles were often seen in walls of neighbouring cells, either marking extended regions of even thickness (e.g., Supporting Information S1: Figure 1L,N) or dome-shaped appositions restricted to individual sites (Supporting Information S1: Figure 1K,O–P). There was no marked difference in the overall callose deposition pattern seen in flg22-treated Col-0 or untreated *mlo2 mlo6 mlo12* mutant leaves. Similarly, the regions of callose deposition were indistinguishable in both genotypes with the typical appearance of electron-dense inclusions in a more electron-translucent matrix; in both genotypes the dome-shaped cell wall appositions were continuously labelled with gold particles. In summary, we conclude that flg22-induced and spontaneously occurring callose-containing cell wall appositions are indistinguishable regarding morphology, ultrastructure and subcellular distribution, suggesting that they are likely synthesised by the same cellular machinery. Additional mutant analysis will, however, be required to substantiate this notion.

2.2 | Plant crowding enhances the pleiotropic phenotypes in *A. thaliana mlo2* and *mlo2 mlo6 mlo12* mutant plants

During routine bulk propagation of plants for seed production, we noticed that *A. thaliana mlo2*-6 single and *mlo2*-6 *mlo6*-4 *mlo12*-8 triple mutant plants consistently showed stronger rosette leaf chlorosis and necrosis when grown at a higher number of plants per pot. Based on this observation, we speculated that higher plant densities might promote this phenotype, possibly because of stress imposed by plant crowding. To test this notion systematically, we set up controlled experiments in which we grew a defined number of plants (either $2 \times 2 = 4$, $3 \times 3 = 9$, or $4 \times 4 = 16$) per pot and monitored the occurrence of chlorosis and necrosis in their rosette leaves over time. At 8 weeks after sowing, leaves of Col-0 wild type plants were entirely green in the 2×2 setting, showed little accumulation of anthocyanins (indicated by a dark purple-brownish colour in only very few leaves) in the 3×3 arrangement, and exhibited a moderate occurrence of anthocyanins in the 4×4 array, indicative of increasing stress upon crowding (Figure 1a). By contrast, *mlo2*-6 single mutant and *mlo2*-6 *mlo6*-4 *mlo12*-8 triple mutant plants revealed slight chlorosis in the 2×2 grouping, which was strongly exacerbated in the 3×3 and even more in the 4×4 assembly. In addition to chlorosis, especially the *mlo2*-6 *mlo6*-4 *mlo12*-8 triple mutant plants grown in the 4×4 array showed some signs of leaf necrosis. Few leaves of the *mlo* single and to a lesser

extent the triple mutant plants also had recognisable accumulation of anthocyanins in addition to their chlorotic appearance in this setup (Figure 1a). The enhancing effect of plant crowding was similar for the other *mlo2* mutant allele, *mlo2*-5, and the respective *mlo2*-5 *mlo6*-2 *mlo12*-1 triple mutant (Supporting Information S1: Figure 2). We conclude that plant crowding causes stress in Col-0 wild-type plants, leading to anthocyanin accumulation. It also particularly intensifies the leaf chlorosis phenotype of *A. thaliana mlo2* single mutant and *mlo2 mlo6-mlo12* triple mutant plants, with *mlo2 mlo6 mlo12* triple mutant plants tending to show stronger symptoms than *mlo2* single mutant plants. It further seems as if leaf chlorosis is largely dominant over anthocyanin accumulation upon crowding stress in these *mlo* mutants, as they mostly lacked the typical dark purple coloration indicating the presence of anthocyanins.

We next wondered whether elevated plant densities would also promote the occurrence of spontaneous callose-containing cell wall depositions in the *mlo* mutants. At 8 weeks after sowing, we sampled leaves from Col-0 wild-type and *mlo* mutant plants, grown in either 2 × 2 or 4 × 4 settings, and subjected them to Aniline blue staining for the histochemical detection of callose by epifluorescence microscopy. Quantitative assessment of bright fluorescent spots (indicative of callose) in the rosette leaves revealed low numbers (median <1000 cm^{-2}) for Col-0 plants under both conditions. By contrast, in leaves of *mlo2*-6 single mutants and in particular *mlo2*-6 *mlo6*-4 *mlo12*-8 triple mutants, the number of fluorescent spots per area was significantly higher in the 4 × 4 arrangement (median ~1500 cm^{-2} and ~3100 cm^{-2}, respectively) as compared to the 2 × 2 assembly (median ~440 cm^{-2} and ~410 cm^{-2}, respectively (Figure 1b; see also data of two additional experimental replicates in Supporting Information S1: Figure 3, showing a similar trend)). Consistent with the stronger symptoms in *mlo2*-6 *mlo6*-4 *mlo12*-8 triple mutant plants in comparison to *mlo2*-6 single mutant plants regarding leaf chlorosis and necrosis at higher plant densities (Figure 1a), in the 4 × 4 setting the triple mutant plants accumulated higher numbers of fluorescent spots per area in their rosette leaves. This disparity is reminiscent of the differential powdery mildew resistance phenotype seen with *mlo2* single and *mlo2 mlo6 mlo12* triple mutants (Acevedo-Garcia, Gruner, et al., 2017; Consonni et al., 2006). Similar to *mlo2*-6, *mlo2*-5, a second *mlo2* single mutant allele tested, showed more callose spots in the leaves than Col-0 plants, in particular in the 4 × 4 setup (Supporting Information S1: Figure 4). In conclusion, plant crowding not only enhances the macroscopically visible chlorosis/necrosis phenotype of *mlo* mutant plants, but also promotes the spontaneous formation of callose-containing cell wall depositions in leaf mesophyll cells in the tested *A. thaliana* single and triple *mlo* mutant plants.

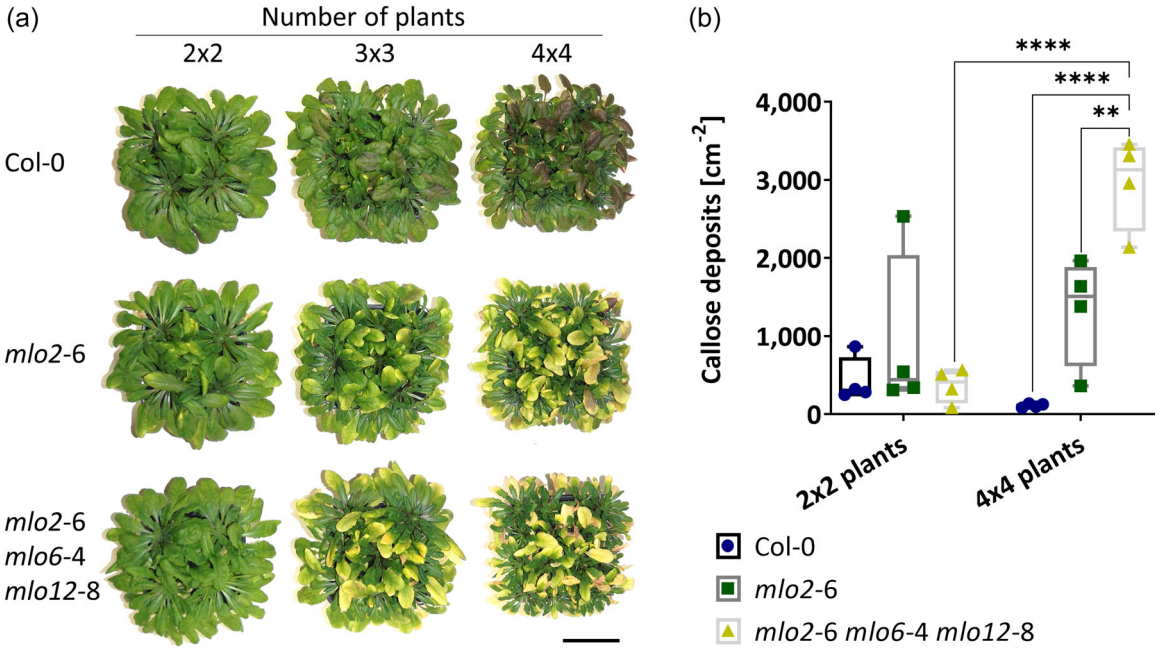

FIGURE 1 Higher growth density increases the development of pleiotropic phenotypes in *Arabidopsis thaliana mlo* mutants. Phenotype of 8-week-old *A. thaliana* wild-type (Col-0) and *mlo2*-6 and *mlo2*-6 *mlo6*-4 *mlo12*-8 mutant plants grown at different densities. (a) Macroscopic phenotype of plants grown with 2 × 2, 3 × 3, and 4 × 4 plants in each pot (i.e., 4, 9 and 16 plants, respectively). The size bar equals 5 cm. The experiment was repeated once with a similar outcome. (b) Callose depositions per area in mature rosette leaves of the indicated genotypes from the 2 × 2 and 4 × 4 settings of the experiment shown in (a). Data are based on $n = 1$ experimental replicate with four leaves from different plants. For statistical analysis, a two-way analysis of variance with multiple comparisons test (**$\alpha = 0.005$, ****$\alpha = 0.0001$) was performed. See also data of two additional experimental replicates in Supporting Information S1: Figure 3.

2.3 | Fertilisation relieves the intensification of chlorosis and necrosis in rosette leaves of *A. thaliana mlo2* and *mlo2 mlo6 mlo12* mutants triggered by plant crowding

We speculated that the enhancement of the pleiotropic *mlo* mutant phenotypes under crowding stress might be based on reduced nutrient availability due to between-plant competitions in these conditions. To test this hypothesis experimentally, the crowding experiment described above (Figure 1a) was repeated with one set of pots being supplied with commercial mineral fertiliser (0.2% Wuxal® universal liquid fertiliser) at 3 and 5 weeks after sowing, with plants being assessed at an age of 8 weeks. Overall, the fertilisation regime led to more vigorous plants across all genotypes, harbouring more and larger rosette leaves than their non-fertilised counterparts of the same age. It further caused a strong suppression or delay of the chlorotic/necrotic phenotype in *mlo2*-6 single mutant and *mlo2*-6 *mlo6*-4 *mlo12*-8 triple mutant plants (Figure 2a). The fertilised mutant plants showed only weak signs of leaf chlorosis at the edges (mostly the tips) of some rosette leaves. Fertilisation also largely suppressed or delayed the accumulation of anthocyanins in the rosette leaves of Col-0 wild-type plants (Figure 2a), indicating a release from stress. The effect of fertilisation lasted up to a plant age of at least ten weeks (Supporting Information S1: Figure 5).

Other than in the experiment described above, in this trial also *mlo* mutant plants grown in the 2 × 2 setting revealed some leaf chlorosis and necrosis at the age of 8 weeks, highlighting the typical variation in the onset of this phenotype (cf. Figure 1a and Figure 2a; see also Consonni et al., 2006).

Given that fertilisation largely rescued the chlorosis/necrosis phenotype in rosette leaves of *A. thaliana mlo* mutants, we wondered whether it would also alleviate the occurrence of the spontaneous callose-rich depositions in the leaf cells of these plants. Col-0 control plants exhibited similarly low numbers of fluorescent spots (median <500 cm^{-2}) in the absence or presence Wuxal®. By contrast, in leaves of *mlo2*-6 single mutants and in particular *mlo2*-6 *mlo6*-4 *mlo12*-8 triple mutants, the number of fluorescent spots was elevated in densely grown (4 × 4 setup) non-fertilised plants (median ~2800 cm^{-2} and ~4400 cm^{-2}, respectively), as seen before (cf. Figure 1b). Unexpectedly, however, we found similar numbers of fluorescent spots per area in fertilised *mlo* mutant plants (median ~1900 cm^{-2} and ~5400 cm^{-2}, respectively; Figure 2b; see also data of two additional experimental replicates in Supporting Information S1: Figure 3, showing a similar trend). This finding indicates that fertilisation uncouples the macroscopically recognisable chlorosis/necrosis phenotype of *A. thaliana mlo* mutants from the spontaneous formation of callose-rich cell wall depositions in these lines.

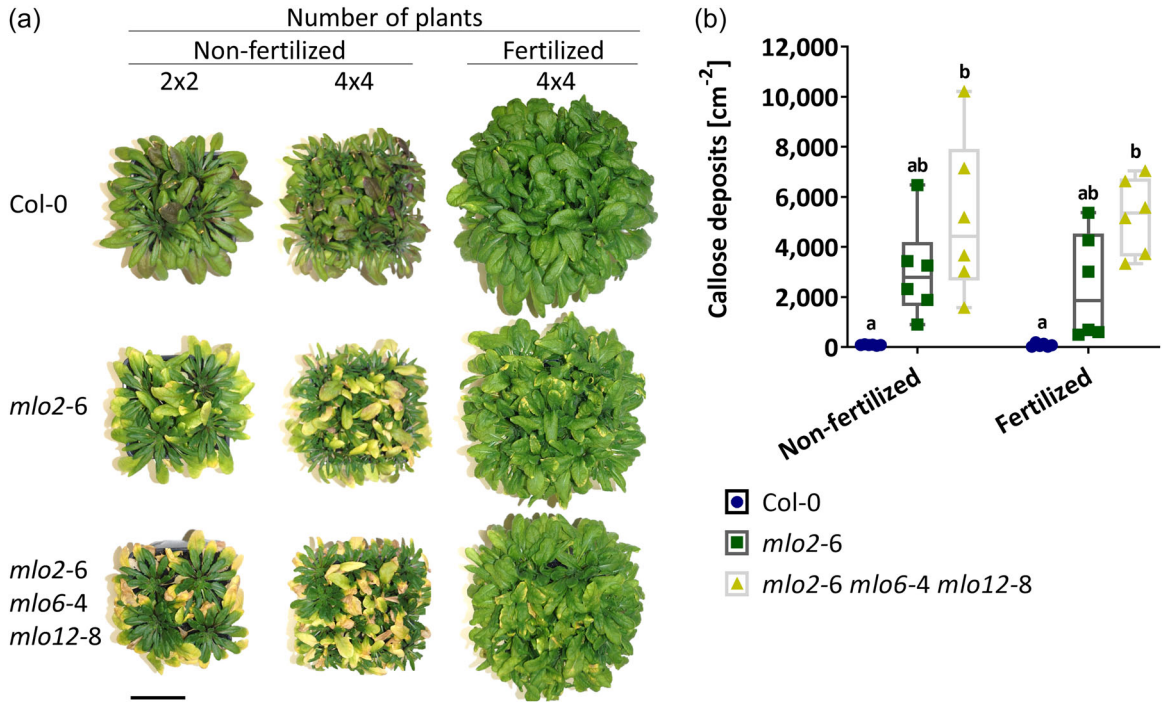

FIGURE 2 Fertilisation relieves signs of early leaf senescence but not spontaneous callose depositions in *Arabidopsis thaliana mlo* mutants. Phenotype of 8-week-old *A. thaliana* wild-type (Col-0) and *mlo2*-6 and *mlo2*-6 *mlo6*-4 *mlo12*-8 mutant plants grown at different densities and without or with the application of fertiliser. (a) Macroscopic phenotype of plants grown with 2 × 2 and 4 × 4 plants per pot either with or without fertilisation. Fertilisation was added as 0.2% liquid Wuxal® universal fertiliser at the plant age of 3 and 5 weeks. The size bar equals 5 cm. The experiment was repeated once with a similar outcome. (b) Callose depositions per area in mature rosette leaves of the genotypes grown in the 4×4 arrangement from the experiment shown in (a). Data are based on $n = 1$ experimental replicate with six leaves from different plants. For statistical analysis, a two-way analysis of variance with Sidak's multiple comparisons test (***$\alpha = 0.001$) was performed. See also data of two additional experimental replicates in Supporting Information S1: Figure 2. [Color figure can be viewed at wileyonlinelibrary.com]

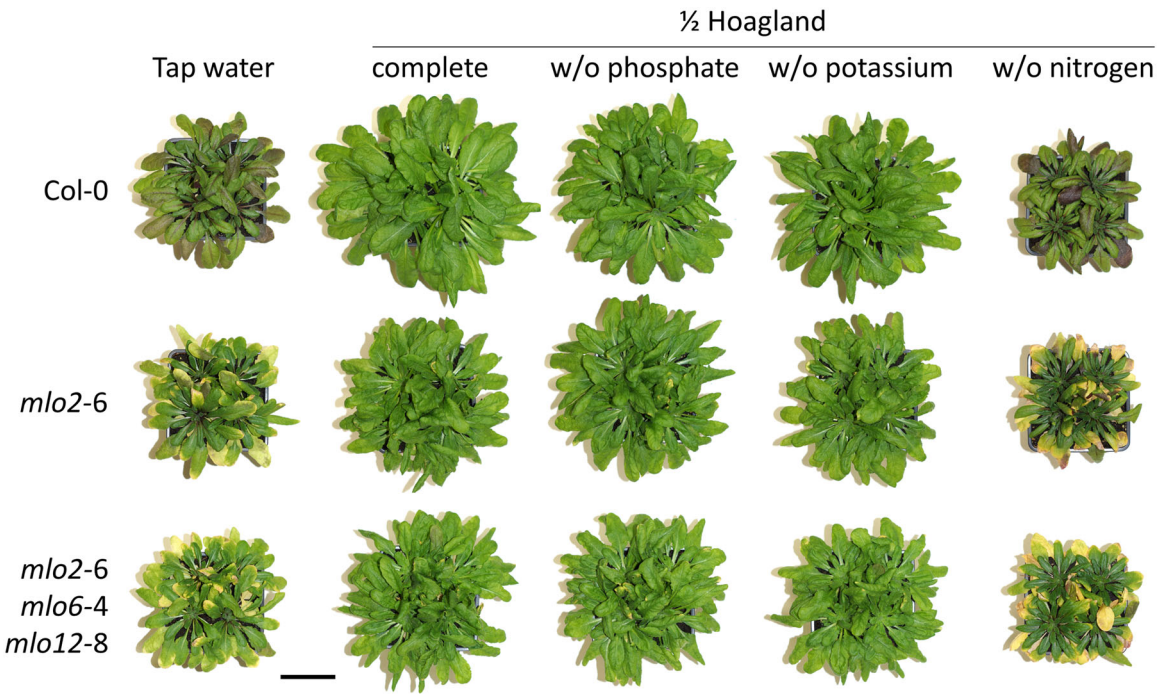

FIGURE 3 Nitrogen deficiency is a key determinant of the pleiotropic phenotypes associated with *Arabidopsis thaliana mlo* mutants. Phenotype of 7-week-old *A. thaliana* wild-type (Col-0) and *mlo2-6* and *mlo2-6 mlo6-4 mlo12-8* mutant plants watered either with tap water or with different ½ Hoagland solutions (including all nutrients or missing one of the three macro-nutrients nitrogen, phosphate or potassium as indicated). The size bar equals 5 cm. The experiment was repeated twice with a similar outcome. [Color figure can be viewed at wileyonlinelibrary.com]

To further elucidate which component of the liquid mineral fertiliser is responsible for the suppression of the early leaf senescence in *A. thaliana mlo* mutant plants, we next conducted controlled growth experiments with differential nutrient supplementation. Therefore, the same genotypes as used before (Col-0, *mlo2-6* single mutant and *mlo2-6 mlo6-4 mlo12-8* triple mutant) were continuously watered with different ½ Hoagland solutions, either containing all nutrients or missing one of the three macronutrients nitrogen, phosphate or potassium. Watering with the complete ½ Hoagland solution expectedly led to a similarly relieved phenotype in the case of *mlo2-6* and *mlo2-6 mlo6-4 mlo12-8* mutant plants as achieved by application of the liquid mineral fertilisation in the previous experiment (Figure 2a). The same was true for treatment with the compositions lacking phosphate or potassium. By contrast, the *mlo* mutant plants that were supplied with ½ Hoagland lacking nitrogen displayed a strong senescence phenotype comparable to the tap water control (Figure 3). This outcome hints towards the development of the senescence phenotype being linked to the plant's nitrogen metabolism.

2.4 | Fertilisation also reduces the development of chlorotic/necrotic lesions in leaves of a barley *mlo* mutant

As liquid mineral fertilisation prevented or delayed the occurrence of leaf chlorosis and necrosis in rosette leaves of *A. thaliana mlo* mutants, we wondered whether the same might be true in the case of barley. To address this question, we focused on the back-cross Ingrid (BCI) *mlo*-3 mutant, which reproducibly exhibits lesions in primary leaves (Gruner et al., 2020; Wolter et al., 1993). The *mlo*-3 allele was chosen from an array of different barley *mlo* mutant alleles (BCI *mlo*-1 to *mlo*-11) as it showed the strongest pleiotropic phenotypes under our growth conditions (Supporting Information S1: Figure 6). We analysed primary leaves of wild type (cv. Ingrid; *Mlo* genotype) and BCI *mlo*-3 plants with respect to the extent of necrotic leaf area by automated image analysis at 17 days and 21 days after sowing, in both the absence and presence of liquid fertilisation. At 17 days after sowing, leaves of non-fertilised BCI *mlo*-3 mutant plants exhibited extensive chlorosis and numerous discrete necrotic spots scattered along the leaf blade (Figure 4a), resulting in a median of ~5% necrotic leaf area (Figure 4b). Similar to *A. thaliana mlo* mutants (Figure 2), this phenotype was strongly diminished upon the application of Wuxal® (0.2%). At 21 days after sowing, the necrotic area increased to approximately 53% (median) in leaves of non-fertilised BCI *mlo*-3 mutant plants and was again lower (median ~10%) upon fertilisation (Figure 4b). We conclude that the effect of nutrition on the relief of *mlo*-conditioned leaf chlorosis and necrosis is similar in mono-cotyledonous (barley) and dicotyledonous (*A. thaliana*) plants.

In the course of our experiments, we also noticed that the extent of necrotic leaf area in leaves of the BCI *mlo*-3 mutant varied with soil type. We analysed this aspect quantitatively at 21 days after sowing in three representative soil types – "SoMi513", "Dachgarten Extensiv"

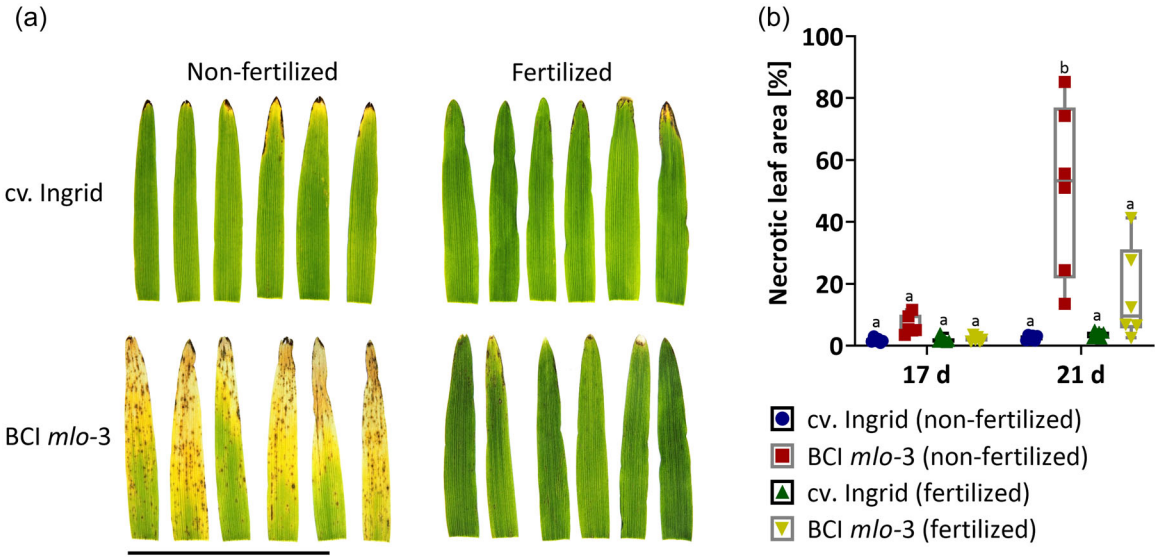

FIGURE 4 Fertilisation relieves signs of early leaf senescence and spontaneous occurrence of chlorosis and the formation of necrotic lesions in the barley BCI *mlo*-3 mutant. (a) Macroscopic phenotype of primary leaves from both barley lines at 17 days after sowing, grown either without fertilisation (left) or with fertilisation (right). Fertilisation was supplied as 0.2% liquid Wuxal® universal fertiliser at around 1 week after sowing. The size bar equals 5 cm. The experiment was repeated five times with a similar outcome. (b) Quantification of necrotic leaf area in the apical 5 cm of barley primary leaves of the indicated genotypes, scored at 17 and 21 days after sowing, grown either with or without fertilisation. Plants were grown in the "Dachgarten Extensiv" substrate. Data are based on $n = 6$ experimental replicates with 3–6 leaves per treatment/genotype, time point and replicate. Letters indicate different significance groups based on a two-way analysis of variance with multiple comparisons test ($\alpha = 0.0001$). [Color figure can be viewed at wileyonlinelibrary.com]

and "Bio Topferde", which differ markedly in their nutrient composition (Supporting Information S1: Table 1). BCI *mlo*-3 mutant plants grown in "Dachgarten Extensiv", a nutrient-poor soil, showed a similar phenotype (median ~53% necrotic leaf area) as unfertilised *mlo* mutant plants in the fertiliser experiment described above (Figure 4), which was also performed in this soil. By contrast, the degree of necrosis was substantially lower (median ~31% necrotic leaf area) in "Bio Topferde" and close to the level of wild type (cv. Ingrid) in "SoMi513" soil (~6% necrotic leaf area; Supporting Information S1: Figure 7), two soils with higher nutrient contents. These results indicate that soil type, presumably primarily its nutrient content, is a key determinant for the occurrence and extent of *mlo*-associated pleiotropic phenotypes.

2.5 | The extent of *mlo*-conditioned leaf necrosis in barley is modulated by temperature and light intensity

Next, we aimed to explore how temperature and light intensity may impact the extent of *mlo*-associated leaf chlorosis and necrosis. To study this aspect, we focused on the barley BCI *mlo*-3 mutant and the matching cv. Ingrid wild type, as the pleiotropic phenotypes develop faster in barley than in *A. thaliana mlo* mutant plants, which enabled us to test more conditions within a reasonable time frame. We grew cv. Ingrid and BCI *mlo*-3 plants in time-course experiments in eight out of nine possible combinations of three different temperatures (15, 20, and 25°C) and three different light conditions (65, 150, and 250 µmol $m^{-2}\,s^{-1}$), with 20°C in combination with 150 µmol $m^{-2}\,s^{-1}$ being our standard condition also used in other experiments of this study. We excluded the combination of high temperature (25°C) and high light intensity (250 µmol $m^{-2}\,s^{-1}$) from this set of experiments as the joint stress severely impeded plant growth. As overall plant development is influenced by light and temperature, depending on the respective combination, 3–5 different time-points were chosen for the automated assessment of leaf necrotic area as described above (cf. Figure 4). However, in the current experiment this parameter turned out to yield data with high variation, especially at elevated temperatures, likely due to extensive plant stress imposed by these conditions (Supporting Information S1: Figure 8). Consequently, the number of necrotic spots was deemed a potentially better indicator for the true effects of light and temperature on *mlo*-mediated necrosis in this experiment. We, therefore, manually quantified the number of necrotic leaf lesions based on the same samples/photos used for the automated evaluation. We observed that the number of necrotic spots slightly decreased from low to high temperature and from low to high light intensity. Accordingly, the highest difference between cv. Ingrid wild type and BCI *mlo*-3 mutant was seen at the combination of low temperature (15°C) and low light intensity (65 µmol $m^{-2}\,s^{-1}$), and the least difference at the combination of high temperature (25°C) and medium light intensity (150 µmol $m^{-2}\,s^{-1}$; Figure 5; note that we did not test high temperature in combination with high light intensity – see above). Thus, we conclude that elevated temperatures and higher light intensities, alone or in combination, suppress or delay the necrotic leaf spot phenotype of the BCI *mlo*-3 mutant.

2.6 | Light irradiation is required for the development of necrotic lesions in the barley BCI *mlo*-3 mutant

In the course of our experiments, we observed that chlorotic and necrotic leaf areas initiate at the leaf tip (i.e., the oldest part of the leaf) and progressively extend towards the leaf base (i.e., the youngest part of the leaf) in barley BCI *mlo*-3 mutant plants (Figure 6a). It is well known from many other plant lesion mimic mutants that light irradiation is required for the development of the characteristic leaf spots (Gray et al., 2002; Ma et al., 2020; Wang et al., 2016; Yuchun et al., 2021; Zhang et al., 2019). To test whether this might be also true for the barley BCI *mlo*-3 mutant, we grew wild-type (cv. Ingrid) and BCI *mlo*-3 mutant plants and either covered their leaf tips with aluminium foil at 14 days after sowing for 3 days or left them uncovered. In the latter case, we observed that BCI *mlo*-3 mutant plants developed the typical leaf chlorosis and speckled necrosis, while the leaves of cv. Ingrid wild-type plants stayed largely green, except for some slight necrosis at the very leaf tips, which is typical for barley plants grown in our conditions (Figure 6a,b). By contrast, coverage with aluminium foil caused some weak chlorosis along the blade and slight brownish necrosis at the very tip of leaves in wild-type (cv. Ingrid) plants. Covered leaves of BCI *mlo*-3 mutant plants also showed a chlorotic blade (with possibly somewhat more intense yellowing than in cv. Ingrid wild-type plants) and brownish necrosis at the very tip, but lacked the majority of the characteristic necrotic spots that are typically scattered densely along the leaf blade (Figure 6a,b). We conclude that direct light irradiance strongly promotes the formation of the typical necrotic spots in leaves of barley BCI *mlo*-3 mutant plants.

To learn more about the light dependence of the *mlo* phenotype we repeated the experiment described above but enclosed only part of the leaves in aluminium foil. Additionally, after 3 days of coverage, we removed the aluminium foil in half of the leaves and grew the plants for another 4 days. This experimental setup resulted in leaves that were either partly covered for 7 days or that were partly enclosed for 3 days and allowed to recover for another 4 days. Leaves of cv. Ingrid wild-type plants that were partly wrapped for 7 days showed segmental chlorosis in the shielded regions that possibly was somewhat more severe than in the previous experiment following 3 days of coverage (Figure 7; cf. Figure 6a). In case of the BCI *mlo*-3 mutant, wrapping in aluminium foil resulted in a chlorotic leaf segment that was similar in appearance to the one in cv. Ingrid wild-type plants. However, the protection from light interestingly

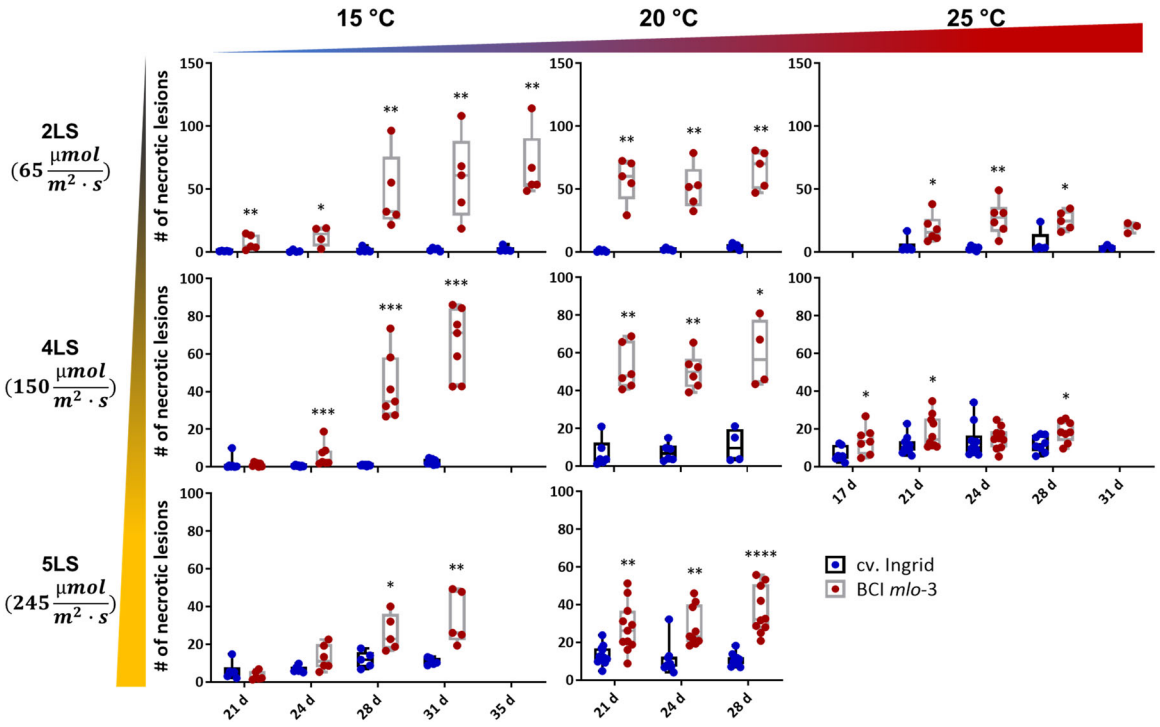

FIGURE 5 Lower temperature and light intensity enhance the number of spontaneous necrotic lesions in primary leaves of the barley BCI *mlo*-3 mutant. Quantification of necrotic lesions in the apical 5 cm of cv. Ingrid and BCI *mlo-3* primary leaves grown under different combinations of temperature and light intensity. Plants were grown in the "Dachgarten Extensiv" substrate in a closed light-cabinet (Panasonic MLR-352) set to 15, 20 or 25°C in combination with low (65 µmol m^{-2} s^{-1}), medium (150 µmol m^{-2} s^{-1}) or high (250 µmol m^{-2} s^{-1}) light intensity. Primary leaves were harvested at 17–35 days and the number of necrotic lesions in the apical 5 cm of the leaves was quantified. Data are based on n = 3–11 experimental replicates, with six leaves per setting combination, genotype, time point and replicate. For statistical analysis, a Mann–Whitney test (*α = 0.05; **α = 0.005; ***α = 0.001; ****α = 0.0001) was performed in which each value of BCI *mlo-3* was compared to the respective value of cv. Ingrid for the same setting and time point. Note the different y-axis scales for the different light intensities. [Color figure can be viewed at wileyonlinelibrary.com]

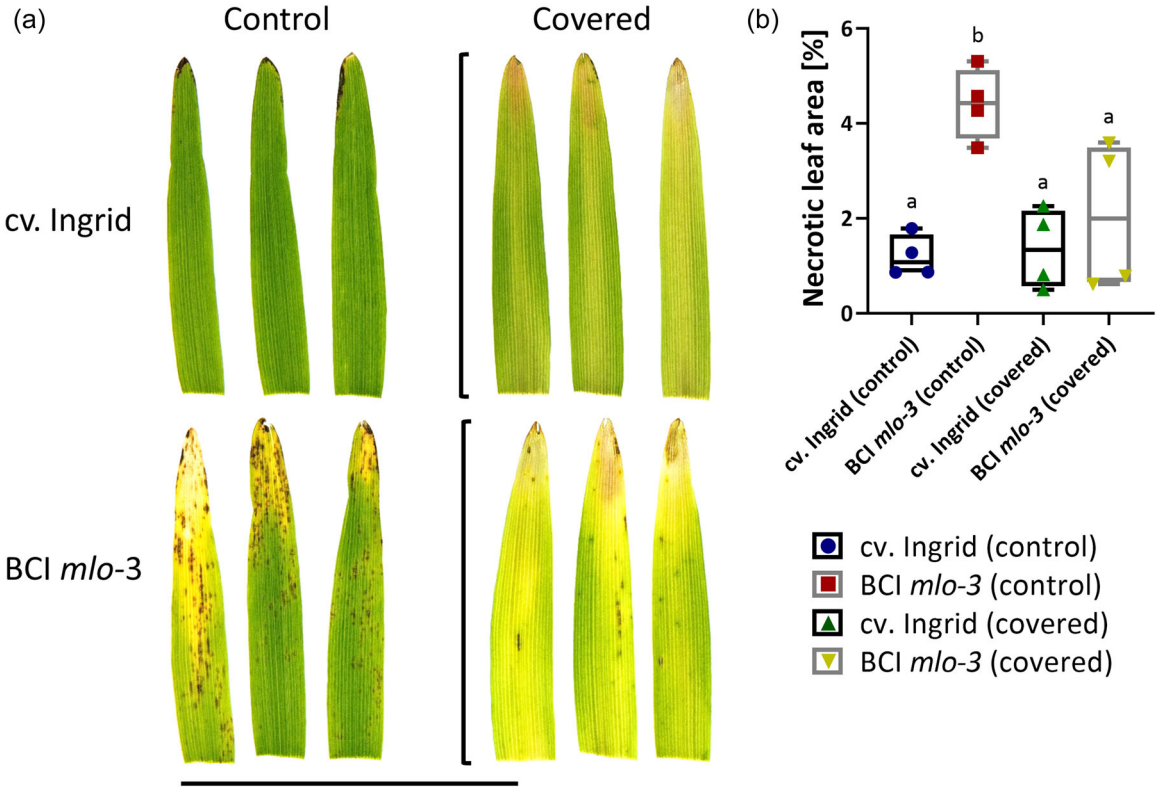

FIGURE 6 Direct irradiance is required for the development of necrotic lesions in the barley BCI *mlo*-3 mutant. (a) Phenotype of 17-day-old primary barley leaves of cv. Ingrid and BCI *mlo*-3 without (control, left) or with covering (right) of the apical leaf part with aluminium foil for 3 days before the evaluation (indicated by the square brackets). The size bar equals 5 cm. The experiment was repeated three times with a similar outcome. (b) Quantification of necrotic leaf area in the apical 5 cm of barley primary leaves of the indicated genotypes, grown either uncovered (control) or covered with aluminium foil as shown in (a). Plants were grown in the "Dachgarten Extensiv" substrate. Data are based on $n = 4$ experimental replicates with 3–6 leaves per treatment/genotype and replicate. Letters indicate different significance groups based on an ordinary one-way analysis of variance with multiple comparisons test ($\alpha = 0.05$). [Color figure can be viewed at wileyonlinelibrary.com]

resulted in an interruption in the formation of necrotic leaf spots, which commenced at the leaf tip, was intersected by the chlorotic (covered) area, and continued thereafter towards the leaf base (Figure 7). Notably, in the BCI *mlo*-3 leaf samples that were allowed to recover for 4 days following enclosure for 3 days, some necrotic spots developed in the previously shielded, chlorotic regions (Figure 7). These findings further underline the intensifying effect of light regarding the formation of the typical necrotic spots in leaves of barley BCI *mlo*-3 mutant plants, similarly as described previously for lesion-mimic mutants in various plant species (Ma et al., 2020; Wang et al., 2015, 2016; reviewed in Freh et al., 2022).

3 | DISCUSSION

Angiosperm plants with mutational lesions in dedicated *Mlo*/*MLO* genes exhibit durable broad-spectrum resistance against powdery mildew infection, which can be considered a powerful universal weapon to combat this fungal disease (Kusch & Panstruga, 2017). However, the deployment of *mlo* mutants in agriculture is in part limited due to the occurrence of the pleiotropic phenotypes associated with these mutants. This shortcoming has initially hindered the widespread use of barley *mlo* mutant plants in farming, though nowadays spring barley *mlo* elite varieties are widely grown in Europe (Dreiseitl, 2022; Lyngkjær et al., 2000). According to various anecdotal reports and our own observations, the occurrence of chlorotic and necrotic leaf lesions in barley *mlo* mutants is generally robust and reproducible, yet seems to vary due to so far unrecognised factors. We here undertook a first attempt to characterise the parameters that may influence the occurrence and extent of the pleiotropic phenotypes in representative dicotyledonous (*A. thaliana*) and monocotyledonous (barley) *mlo* mutant plants. For practical reasons, we performed some assays of this study only with *A. thaliana mlo* mutant plants (e.g. the ultrastructural analysis of callose depositions and crowding experiments; Figures 1–3 and Supporting Information S1: Figure 1), while others were conducted solely with barley *mlo* mutants (e.g. light and temperature experiments; Figures 5–7 and Supporting Information S1: Figure 8). We feel, however, that the synopsis of the generated data set enabled a general overview regarding the factors that govern the development of the early leaf senescence syndrome associated with these mutants.

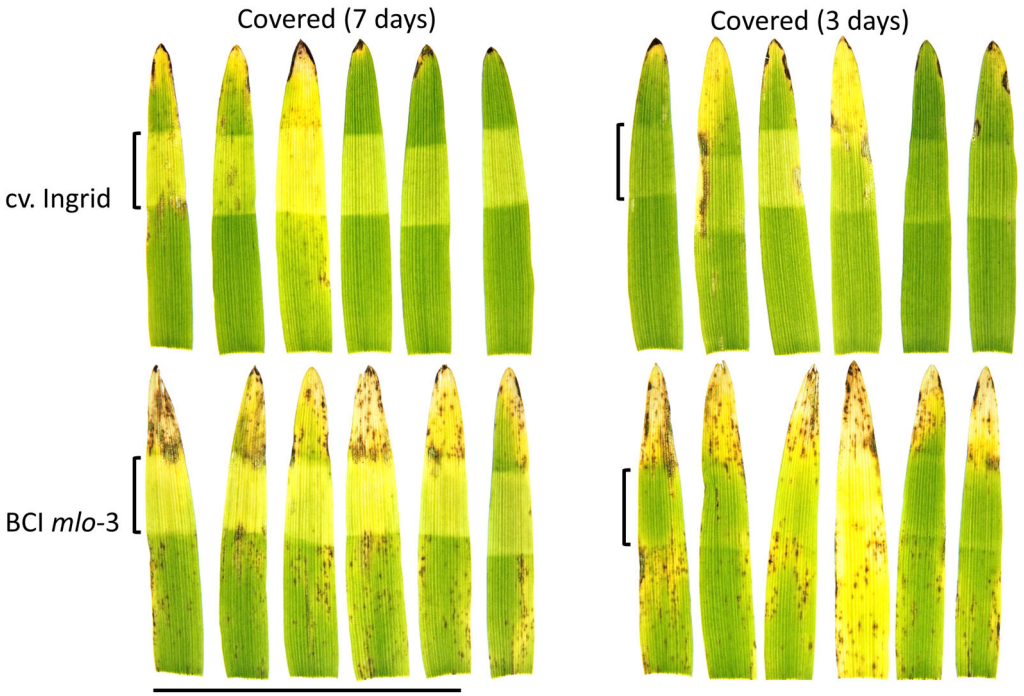

FIGURE 7 Progression of necrotic lesion formation from the leaf tip is not prevented by partial leaf covering. Phenotype of 21-day-old primary barley leaves that were partially covered with aluminium foil in the central leaf region (indicated by the square brackets) from 14 days on. Leaves shown on the left side stayed covered for 7 days, the covering from the leaves on the right side were removed after 3 days. Plants were grown in the "Dachgarten Extensiv" substrate. The size bar equals 5 cm. The 7-day partial leaf covering experiment was repeated once with a similar outcome, the 3-day partial covering experiment could not be reproduced due to an earlier onset of senescence in the following experiments. [Color figure can be viewed at wileyonlinelibrary.com]

We found that plant growth density (Figure 1 and Supporting Information S1: Figures 2–5) and nutrient availability (Figures 2–4 and Supporting Information S1: Figures 3 and 5) are major factors influencing leaf chlorosis and necrosis of *mlo* mutants, while the impact of light intensity and temperature (Figure 5 and Supporting Information S1: Figure 8) turned out to be less severe. The marked effect of growth density and nutrient availability is likely to be interdependent: Higher plant densities cause, amongst other effects, competition for nutrients, thereby limiting nutrient access per individual plant. Neighbouring plants are known to compete for resources such as nutrients, water and light in natural settings, which can generate stress in densely growing plants (Craine & Dybzinski, 2013). The enhanced development of leaf chlorosis and necrosis seen for *A. thaliana mlo* mutant plants upon crowding (Figure 1) is thus likely a direct consequence of the limited nutrient resources available per individual plant when grown in such a regime. This notion is further supported by the fact that application of a liquid mineral fertiliser relieved the pleiotropic phenotypes (Figures 2 and 3), rendering it unlikely that exaggerated aboveground contacts between neighbouring plants is the primary reason for the enhanced leaf chlorosis and necrosis of these *mlo* mutants when densely grown. Plant crowding nonetheless also generated stress for Col-0 wild-type plants, as could be seen from the accumulation of anthocyanins in rosette leaves in these conditions. However, unlike as for *mlo* mutant plants, in Col-0 plants this stress did not translate into an early senescence programme and accelerated leaf decay (Figure 1).

Based on controlled fertilisation experiments, we identified nitrogen as the macronutrient whose deficiency in the growth substrate triggers the onset of pleiotropic phenotypes in the *A. thaliana mlo* mutants (Figure 3). This finding is consistent with the observation that barley BCI *mlo*-3 mutant plants showed the least signs of leaf chlorosis and necrosis in a soil type with high nitrogen content (Supporting Information S1: Figure 7 and Table 1). Notably, nitrogen deficiency is well known to induce early leaf senescence in *A. thaliana* (Fan et al., 2023; Wen et al., 2020). Other Arabidopsis mutants such as the *nla* mutant, which is defective in a gene encoding a RING-type ubiquitin ligase, and the *gds1* mutant, lacking a functional transcription factor regulating the expression of senescence-associated genes, also exhibit early leaf senescence upon growth in nitrogen-limiting conditions (Fan et al., 2023; Peng et al., 2007). It seems as if these mutants as well as *mlo* mutant plants are hypersensitive to nutritional stress. Similar to the *mlo* pleiotropic effects, constitutive and induced levels of trypsin inhibitors were significantly reduced by intraspecific competition in a density-dependent manner in *Brassica napus*—a crowding phenotype that notably likewise could be rescued by nutrient addition (Cipollini & Bergelson, 2001).

Although the effect of nitrogen deficiency on the onset of plant senescence is incompletely understood, various mechanisms have

been discussed. These include the role of nitrogen in amino acid and chlorophyll biosynthesis as well as the interaction of the nitrogen metabolism with phytohormones that regulate plant senescence, such as auxin, cytokinin, ethylene and abscisic acid (Wen et al., 2020). However, it remains unknown which of these factors is linked to the rescue of the *mlo* senescence phenotype by exogenous nitrogen supply. Even though our analyses strongly point to a key role of nutrient richness as an essential component determining the extent of pleiotropic phenotypes in soil-grown barley *mlo* mutant plants (Supporting Information S1: Figure 7 and Table 1), we appreciate that other soil features may also contribute. Abiotic and biotic characteristics such as the geochemical soil structure (Bronick & Lal, 2005) and the composition of soil microbiota (Custódio et al., 2022), respectively, may further modulate the occurrence of pleiotropic phenotypes associated with *mlo* mutants. As nitrogen supply seems to be a critical factor, the association with microbes linked to the acquisition of inorganic and organic sources of nitrogen, such as symbiotic rhizobial bacteria and arbuscular mycorrhizal fungi, which in turn is also linked to soil type (Evans et al., 1993; Oehl et al., 2010), could be essential. Indeed, barley *mlo* mutants were found to be impaired during the early establishment of symbiosis with arbuscular mycorrhizal fungi (Jacott et al., 2020) and the accommodation of the beneficial root endophyte *Serendipita indica* (syn. *Piriformospora indica*) (Hilbert et al., 2020), which may affect nutrient acquisition by these mutants. Given these considerations, it remains to be tested whether fertilisation also relieves *mlo*-associated premature leaf senescence under different field conditions.

At the mechanistic level, the biochemical function of MLO proteins as calcium channels (Gao et al., 2022, 2023) might be linked to the factors modulating the pleiotropic *mlo* phenotypes. For example, calcium signalling networks are known to mediate nitrate sensing (Liu, Gao, et al., 2021; Riveras et al., 2015) and adjust the plant's primary nitrate response (Liu et al., 2020). A recognised regulatory module in this context is comprised of the cyclic nucleotide-gated channel protein CGNC15 and the nitrate transceptor NRT1.1, which together control calcium influx from the extracellular space in a nitrate-dependent manner, thereby coupling nutrient status to a specific calcium signature (Wang et al., 2021). Likewise, there is a tight connection between (blue) light perception via phototropins and calcium signalling (Harada & Shimazaki, 2007). It is conceivable that additional components contribute to the complex interplay of nutrient/light sensing and calcium-mediated signal transduction, possibly also involving members of the MLO family. However, further studies are required to substantiate this notion.

It is remarkable that the disease resistance phenotype of *mlo* mutants is very robust and to the best of our knowledge neither dependent on plant age nor on environmental conditions while the pleiotropic phenotypes of these mutants are developmentally controlled (Consonni et al., 2006, 2010; Wolter et al., 1993) and modulated by environmental factors (Figures 1–5). This discrepancy might be best explained by at least two separate signalling pathways triggered by the lack of the respective *Mlo*/*MLO* genes. While one signalling pathway results in penetration resistance to powdery mildew attack, the other causes premature leaf chlorosis and necrosis. This notion is further supported by the largely independent genetic requirements for the two phenotypes in *A. thaliana*: While the pleiotropic phenotypes of the *mlo2* mutant rely on SA signalling and accumulation (Consonni et al., 2006, 2010) and the callose synthase PMR4 (Consonni et al., 2010), powdery mildew resistance rests on *PEN* genes (Consonni et al., 2006) and the biosynthesis of indolic defence metabolites (Consonni et al., 2010). It, therefore, appears as if the two traits can be geneticaly uncoupled. However, this separation seems to be incomplete and/or to depend on the plant species or developmental stage: Barley *mlo ror1* and *mlo ror2* double mutants exhibit both reduced powdery mildew resistance and less spontaneous mesophyll cell death than the parental *mlo* single mutant (Peterhansel et al., 1997). Further molecular and genetic analyses are thus required to complete the picture.

We can only speculate why pleiotropic phenotypes associated with powdery mildew-resistant *mlo* mutants are highly evident in barley (Bjørnstad & Aastveit, 1990; Piffanelli et al., 2002; Schwarzbach, 1976), wheat (Acevedo-Garcia, Spencer, et al., 2017) and *A. thaliana* (Consonni et al., 2006, 2010), but were not seen so far in other plant species harbouring lesions in *MLO* genes, including pea (Humphry et al., 2011), tomato (Bai et al., 2008) and others (Kusch & Panstruga, 2017). Given our findings obtained in the present study, this may relate to the conditions used for plant growth, in particular soil type and fertilisation. Alternatively, or in addition, other plant species might not be as highly sensitised to deficiencies in nutrient supply translating into an early senescence syndrome. Finally, the observed differences might be related to the extent the various plant species engage in interactions with beneficial microbes. While *A. thaliana* is non-symbiotic (Veiga et al., 2013), the colonisation of cereals such as barley and wheat by arbuscular mycorrhizal fungi is variable and cultivar-dependent (Boyetchko & Tewari, 1995; García de León et al., 2020). By contrast, tomato and pea readily engage in mycorrhizal symbiosis, and pea additionally undergoes symbiosis with nitrogen-fixing bacteria. The association of these plant species with beneficial microbes might be further modulated by soil type and fertilisation, adding additional complexity. In any way, further experiments with *mlo* mutants of these species under varied growth conditions will be necessary to address this conundrum.

4 | MATERIALS AND METHODS

4.1 | Plant material

We used *A. thaliana* ecotype Col-0 (wild-type) and the following T-DNA or transposon insertion mutants (all in Col-0 genetic background) for our experiments: *mlo2-6* (Consonni et al., 2006), *mlo2-5 mlo6-2 mlo12-1* (Consonni et al., 2006), *mlo2-6 mlo6-4 mlo12-8* (Acevedo-Garcia, Gruner, et al., 2017). For experiments with barley, we used cv. Ingrid (*Mlo* wild-type) and a panel of *mlo* mutants (*mlo-1* to *mlo-11*), each seven times backcrossed to cv. Ingrid (Büschges et al., 1997; Hinze et al., 1991; Reinstädler et al., 2010).

4.2 | Plant growth conditions

A. thaliana plants were grown under short-day conditions (10 h light period) at 23/20°C day/night and approximately 135 µmol·s^{-1}·m^{-2} irradiance in "Dachgarten Extensiv" (Hawita) or "Einheitserde VM800" (Einheitserdewerke Werkverband e.V., Sinntal-Altengronau) substrates. The different phenotypes were monitored starting from 6 weeks after sowing up to 10 weeks. In the fertilisation setup, plants were supplied with 0.2% Wuxal® (Hauert MANNA Düngerwerke GmbH) liquid universal fertiliser at 3 and 5 weeks after sowing. For the nutrient differentiation experiments, plants were grown in "Einheitserde VM800" and continuously watered with the respective modified ½ Hoagland solutions (Supporting Information S1: Table 2), modified from (Heeg et al., 2008), starting at 2 weeks of plant age. The phenotypes were then evaluated at 7 weeks. Barley plants for the different light and temperature combination experiments were grown in a Panasonic MLR-352 climate control cabinet (PHC Europe B.V.) set to constant 15, 20 or 25°C and 16 h photoperiod of approx. 65, 150 or 245 µmol·s^{-1}·m^{-2} irradiance in the "Dachgarten Extensiv" substrate. All other barley plants were grown in a long-day plant chamber with 16 h light period of approx. 150 µmol·s^{-1}·m^{-2} irradiance at constant 20°C in the same substrate unless noted otherwise. Primary leaves of barley plants were removed from the plants between 17 and 35 days, depending on the setup of each experiment, and subsequently photographed. For the fertilisation experiment, the plants were supplied with 0.2% Wuxal® liquid universal fertiliser 1 week after sowing. For the covering experiments, the marked areas were covered 3 days before the estimated development of the phenotype with either aluminium foil or coloured plastic foil (Leitz 4100 document hull; LEITZ ACCO Brands GmbH & Co. KG).

4.3 | Quantification of spontaneous callose-containing cell wall depositions in *A. thaliana*

Four to six detached *A. thaliana* leaves per genotype were placed in 80% ethanol for fixation and de-staining. After complete de-staining of the leaves, they were transferred to a 0.05% (w/v) Aniline blue solution (in 67 mM K_2HPO_3, pH 5.8) and incubated for at least 24 h. The samples were then evaluated using a Keyence BZ-9000 epifluorescence microscope (KEYENCE Deutschland GmbH) with the DAPI filter set (excitation λ = 370 nm, emission λ = 509 nm). To this end, two pictures were taken in randomly chosen areas of every leaf. The number of callose-containing cell wall depositions was determined with the Cell Profiler software (Jones et al., 2008).

4.4 | Assessment of necrotic area in primary barley leaves

The detached barley leaves were photographed on a Kaiser slimlite light plate (Kaiser Fototechnik GmbH & Co. KG) to minimise background. Single leaves were subsequently analysed for the relative necrotic leaf area using the leaf necrosis classifier software (https://www.quantitative-plant.org/software/leaf-necrosis-classifier). For this purpose, the datasets for neural network formation were trained manually with pictures from the experiments and optimised for the different setups. To quantify the number of necrotic lesions the same leaf pictures were evaluated manually, as the software was not able to resolve multiple lesions that developed in close proximity (confluent lesions).

4.5 | Immunodetection of callose by light and transmission electron microscopy

A. thaliana rosette leaf samples for resin embedding and subsequent immunocytochemical analysis were excised from Col-0 wild-type and *mlo2*-5 *mlo6*-2 *mlo12*-1 mutant plants grown for 7 weeks in short-day conditions. Before sampling, two mature rosette leaves of four plants (i.e., eight leaves in total) were infiltrated on the lower (abaxial) side with flg22 (Centic Biotec), two leaves of another four plants were infiltrated with water (mock treatment), while leaves of another four plants remained untreated. In the case of the *mlo* triple mutant plants, all leaves remained untreated. The next day, leaves were harvested and split longitudinally into two halves with one half of each leaf subjected to histochemical Aniline blue staining (0.01% (w/v) Aniline blue in 150 mM K_2HPO_4) and subsequent epifluorescence microscopy as described above. The second half of each leaf was cut into approx. 5 mm × 5 mm pieces and chemically fixed, dehydrated and embedded into Araldite 502/Embed 812 resin (EMS, 13940) as described previously (Koskela et al., 2018), with the exception that osmium tetroxide was used at a concentration of 0.5%. Leaf halves from Col-0 leaves showing clear absence (mock control and untreated) or presence (flg22) of callose depositions in their corresponding half after Aniline blue staining as well as leaf halves of the *mlo* triple mutant exhibiting the characteristic age-related Aniline blue callose staining pattern in their corresponding half were chosen for subsequent analysis by microscopy.

For immunofluorescence, 1 µm-sections were cut with a Reichert-Jung Ultracut E ultramicrotome (Reichert-Jung, now: Leica Microsystems), dried down onto adhesive diagnostic microscope slides (ER-202W-AD-CE24; Eerie Scientific LLC (Thermo Scientific) and incubated overnight in TRIS-bovine serum albumin (TRIS-BSA) (20 mM TRIS, 15 mM NaN_3, 225 mM NaCl, pH 6.9) buffer supplemented with 1% (w/v) bovine serum albumin (BSA; A3294; Sigma-Aldrich) and 5% goat serum (G9023; Sigma-Aldrich). After rinsing with TRIS-BSA (3× 10 min), sections were subjected to mouse monoclonal anti-ß-1,3-glucan antibodies (400-2; Biosupplies Australia Pty. Ltd.), diluted 1:100 in TRIS-BSA, for 1 h at room temperature. Following three rinses with TRIS-BSA, sections were incubated with goat-anti mouse Alexa Fluor 488 (abcam ab150117) for 1 h at room temperature. Subsequently, sections were rinsed with TRIS-BSA (3× 10 min) and mounted in CitiFluor™ AF1 (E17970-25, Science Services). Brightfield images were taken on the same day with a

Zeiss Axio Imager D1/D2 equipped with a Zeiss AxioCam HR R3 camera using an EC Plan-Neofluar 40x/0.75 M27 objective (Zeiss). For epifluorescence imaging, a 495 nm beam splitter, a 450-490 nm excitation filter and a 500–550 nm emission filter were used.

For immunogold labelling, ultrathin sections (70–90 nm) were cut from the same resin blocks and collected on nickel slot grids as described before (Moran & Rowley, 1987) and immunolabelled according to Micali and co-workers (Micali et al., 2011) with minor modifications (5% [v/v] goat serum in TRIS-BSA for blocking; 1:100 and 1:200 dilution of mouse monoclonal anti-ß-1,3-glucan antibodies in TRIS-BSA). After staining with 0.1% $KMnO_4$ in 0.1 N H_2SO_4 (Sawaguchi et al., 2001), sections were analysed and imaged using a Hitachi H-7650 transmission electron microscope (Hitachi,) at 100 kV equipped with an AMT XR41-M digital camera (Advanced Microscopy Techniques, Corp.).

4.6 | Statistics

Depending on the experiment, data was analysed with analysis of variances, including multiple comparisons tests or Mann–Whitney tests to compare multiple groups or to compare only the *mlo* mutants to the Col-0 or cv. Ingrid control, respectively. Significance levels are given in the respective Figure legends.

ACKNOWLEDGMENTS

We thank Ila Rouhara for excellent technical assistance regarding the preparation of samples for transmission electron microscopy. This work was supported by the Novo Nordisk Foundation grant NNF19OC0056457 (PlantsGoImmune) to R.P. Open Access funding enabled and organized by Projekt DEAL.

CONFLICTS OF INTEREST STATEMENT

The authors declare no conflict of interest.

DATA AVAILABILITY STATEMENT

The authors confirm that the data supporting the findings of this study are available within the article and its supplementary materials.

ORCID

Matthias Freh http://orcid.org/0000-0002-7969-3166
Kira D. Neumann http://orcid.org/0009-0004-2432-0823
Ulla Neumann http://orcid.org/0000-0001-9200-4209
Ralph Panstruga http://orcid.org/0000-0002-3756-8957

REFERENCES

Acevedo-Garcia, J., Gruner, K., Reinstädler, A., Kemen, A., Kemen, E., Cao, L. et al. (2017) The powdery mildew-resistant Arabidopsis *mlo2 mlo6 mlo12* triple mutant displays altered infection phenotypes with diverse types of phytopathogens. *Scientific Reports*, 7(1), 27.

Acevedo-Garcia, J., Spencer, D., Thieron, H., Reinstadler, A., Hammond-Kosack, K., Phillips, A.L. et al. (2017) *mlo*-based powdery mildew resistance in hexaploid bread wheat generated by a non-transgenic TILLING approach. *Plant Biotechnology Journal*, 15(3), 367–378.

Bai, Y., Pavan, S., Zheng, Z., Zappel, N.F., Reinstädler, A., Lotti, C. et al. (2008) Naturally occurring broad-spectrum powdery mildew resistance in a central American tomato accession is caused by loss of *Mlo* function. *Molecular Plant-Microbe Interactions®*, 21(1), 30–39.

Bjørnstad, Å. & Aastveit, K. (1990) Pleiotropic effects on the ml-o mildew resistance gene in barley in different genetical backgrounds. *Euphytica*, 46(3), 217–226.

Boyetchko, S.M. & Tewari, J.P. (1995) Susceptibility of barley cultivars to vesicular-arbuscular mycorrhizal fungi. *Canadian Journal of Plant Science*, 75(1), 269–275.

Bronick, C.J. & Lal, R. (2005) Soil structure and management: a review. *Geoderma*, 124(1–2), 3–22.

Büschges, R., Hollricher, K., Panstruga, R., Simons, G., Wolter, M., Frijters, A. et al. (1997) The barley *Mlo* gene: A novel control element of plant pathogen resistance. *Cell*, 88(5), 695–705.

Cipollini, D.F. & Bergelson, J. (2001) Plant density and nutrient availability constrain constitutive and wound-induced expression of trypsin inhibitors in *Brassica napus*. *Journal of Chemical Ecology*, 27(3), 593–610.

Consonni, C., Bednarek, P., Humphry, M., Francocci, F., Ferrari, S., Harzen, A. et al. (2010) Tryptophan-derived metabolites are required for antifungal defense in the Arabidopsis *mlo2* mutant. *Plant Physiology*, 152(3), 1544–1561.

Consonni, C., Humphry, M.E., Hartmann, H.A., Livaja, M., Durner, J., Westphal, L. et al. (2006) Conserved requirement for a plant host cell protein in powdery mildew pathogenesis. *Nature Genetics*, 38(6), 716–720.

Craine, J.M. & Dybzinski, R. (2013) Mechanisms of plant competition for nutrients, water and light. *Functional Ecology*, 27(4), 833–840.

Cui, F., Wu, H., Safronov, O., Zhang, P., Kumar, R., Kollist, H. et al. (2018) Arabidopsis MLO2 is a negative regulator of sensitivity to extracellular reactive oxygen species. *Plant, Cell & Environment*, 41(4), 782–796.

Custódio, V., Gonin, M., Stabl, G., Bakhoum, N., Oliveira, M.M., Gutjahr, C. et al. (2022) Sculpting the soil microbiota. *The Plant Journal*, 109(3), 508–522.

Dreiseitl, A. (2022) Powdery mildew resistance genes in European barley cultivars registered in the Czech Republic from 2016 to 2020. *Genes*, 13(7), 1274.

Evans, J., Wallace, C. & Dobrowolski, N. (1993) Interaction of soil type and temperature on the survival of *Rhizobium leguminosarum bv. viciae*. *Soil Biology and Biochemistry*, 25(9), 1153–1160.

Fan, H., Quan, S., Ye, Q., Zhang, L., Liu, W., Zhu, N. et al. (2023) A molecular framework underlying low-nitrogen-induced early leaf senescence in *Arabidopsis thaliana*. *Molecular Plant*, 16(4), 756–774.

Freh, M., Gao, J., Petersen, M. & Panstruga, R. (2022) Plant autoimmunity-fresh insights into an old phenomenon. *Plant Physiology*, 188(3), 1419–1434.

Gao, Q., Wang, C., Xi, Y., Shao, Q., Hou, C., Li, L. et al. (2023) RALF signaling pathway activates MLO calcium channels to maintain pollen tube integrity. *Cell Research*, 33(1), 71–79.

Gao, Q., Wang, C., Xi, Y., Shao, Q., Li, L. & Luan, S. (2022) A receptor–channel trio conducts Ca^{2+} signalling for pollen tube reception. *Nature*, 607(7919), 534–539.

García de León, D., Vahter, T., Zobel, M., Koppel, M., Edesi, L., Davison, J. et al. (2020) Different wheat cultivars exhibit variable responses to inoculation with arbuscular mycorrhizal fungi from organic and conventional farms. *PLoS One*, 15(5), e0233878.

Ge, C., Moolhuijzen, P., Hickey, L., Wentzel, E., Deng, W., Dinglasan, E.G. et al. (2020) Physiological changes in barley *mlo-11* powdery mildew resistance conditioned by tandem repeat copy number. *International Journal of Molecular Sciences*, 21(22), 8769.

Ge, X., Deng, W., Lee, Z.Z., Lopez-Ruiz, F.J., Schweizer, P. & Ellwood, S.R. (2016) Tempered *mlo* broad-spectrum resistance to barley powdery mildew in an Ethiopian landrace. *Scientific Reports*, 6, 29558.

Gray, J., Janick-Buckner, D., Buckner, B., Close, P.S. & Johal, G.S. (2002) Light-dependent death of maize *lls1* cells is mediated by mature chloroplasts. *Plant Physiology*, 130(4), 1894–1907.

Gruner, K., Esser, T., Acevedo-Garcia, J., Freh, M., Habig, M., Strugala, R. et al. (2020) Evidence for allele-specific levels of enhanced susceptibility of wheat *mlo* mutants to the hemibiotrophic fungal pathogen *Magnaporthe oryzae* pv. *triticum*. *Genes*, 11(5), 517.

Habekuss, A. & Hentrich, W. (1988) Charakterisierung funktionell verschiedener ml-o-mutanten durch primärinfektion, pustelwachstum, inkubation und befallsverlauf. *Tagungsbericht, Akademie der Landwirtschaftswissenschaften der Deutschen Demokratischen Republik*, 272, 229–237.

Harada, A. & Shimazaki, K. (2007) Phototropins and blue light-dependent calcium signaling in higher plants. *Photochemistry and Photobiology*, 83(1), 102–111.

Heeg, C., Kruse, C., Jost, R., Gutensohn, M., Ruppert, T., Wirtz, M. et al. (2008) Analysis of the *Arabidopsis O*-acetylserine(thiol)lyase gene family demonstrates compartment-specific differences in the regulation of cysteine synthesis. *The Plant Cell*, 20(1), 168–185.

Hentrich, W. (1979) Multiple allelie, pleiotropie und züchterische nutzung mehltauresistenter mutanten des mlo-locus der gerste. *Tagungsbericht, Akademie der Landwirtschaftswissenschaften der Deutschen Demokratischen Republik*, 175, 191–202.

Hentrich, W. & Habekuss, A. (1993) Untersuchungen an heteroallelen mutanten des ml-o locus der sommergerste. *Schriftenreihe VAFB Thüringen*, 1/1993, 61–69.

Hilbert, M., Novero, M., Rovenich, H., Mari, S., Grimm, C., Bonfante, P. et al. (2020) *MLO* differentially regulates barley root colonization by beneficial endophytic and mycorrhizal fungi. *Frontiers in Plant Science*, 10, 9319.

Hinze, K., Thompson, R.D., Ritter, E., Salamini, F. & Schulze-Lefert, P. (1991) Restriction fragment length polymorphism-mediated targeting of the *ml-o* resistance locus in barley (*Hordeum vulgare*). *Proceedings of the National Academy of Sciences of the United States of America*, 88(9), 3691–3695.

Humphry, M., Reinstädler, A., Ivanov, S., Bisseling, T. & Panstruga, R. (2011) Durable broad-spectrum powdery mildew resistance in pea *er1* plants is conferred by natural loss-of-function mutations in *PsMLO1*. *Molecular Plant Pathology*, 12(9), 866–878.

Jacott, C.N., Charpentier, M., Murray, J.D. & Ridout, C.J. (2020) Mildew locus O facilitates colonization by arbuscular mycorrhizal fungi in angiosperms. *New Phytologist*, 227, 343–351.

Jones, T.R., Kang, I.H., Wheeler, D.B., Lindquist, R.A., Papallo, A., Sabatini, D.M. et al. (2008) CellProfiler analyst: data exploration and analysis software for complex image-based screens. *BMC Bioinformatics*, 9, 482.

Jørgensen, I.H. (1992) Discovery, characterization and exploitation of Mlo powdery mildew resistance in barley. *Euphytica*, 63(1–2), 141–152.

Koskela, M.M., Brünje, A., Ivanauskaite, A., Grabsztunowicz, M., Lassowskat, I., Neumann, U. et al. (2018) Chloroplast acetyltransferase NSI is required for state transitions in *Arabidopsis thaliana*. *The Plant Cell*, 30(8), 1695–1709.

Kusch, S. & Panstruga, R. (2017) *mlo*-based resistance: An apparently universal "weapon" to defeat powdery mildew disease. *Molecular Plant-Microbe Interactions®*, 30, 179–189.

Kusch, S., Pesch, L. & Panstruga, R. (2016) Comprehensive phylogenetic analysis sheds light on the diversity and origin of the MLO family of integral membrane proteins. *Genome Biology and Evolution*, 8(3), 878–895.

Li, S., Lin, D., Zhang, Y., Deng, M., Chen, Y., Lv, B. et al. (2022) Genome-edited powdery mildew resistance in wheat without growth penalties. *Nature*, 602(7897), 455–460.

Liu, K.-H., Diener, A., Lin, Z., Liu, C. & Sheen, J. (2020) Primary nitrate responses mediated by calcium signalling and diverse protein phosphorylation. *Journal of Experimental Botany*, 71(15), 4428–4441.

Liu, L., Gao, H., Li, S., Han, Z. & Li, B. (2021a) Calcium signaling networks mediate nitrate sensing and responses in Arabidopsis. *Plant Signaling & Behavior*, 16(10), 1938441.

Liu, M., Braun, U., Takamatsu, S., Hambleton, S., Shoukouhi, P., Bisson, K.R. et al. (2021b) Taxonomic revision of *Blumeria* based on multi-gene DNA sequences, host preferences and morphology. *Mycoscience*, 62(3), 143–165.

Lorek, J., Griebel, T., Jones, A.M., Kuhn, H. & Panstruga, R. (2013) The role of *Arabidopsis* heterotrimeric G-protein subunits in MLO2 function and MAMP-triggered immunity. *Molecular Plant-Microbe Interactions®*, 26(9), 991–1003.

Lyngkjær, M.F., Newton, A.C., Atzema, J.L. & Baker, S.J. (2000) The barley *mlo* gene: an important powdery mildew resistance source. *Agronomie*, 20(7), 745–756.

Ma, J., Yang, S., Wang, D., Tang, K., Feng, X.X. & Feng, X.Z. (2020) Genetic mapping of a light-dependent lesion mimic mutant reveals the function of coproporphyrinogen III oxidase homolog in soybean. *Frontiers in Plant Science*, 11, 557.

Martienssen, R. (1997) Cell death: fatal induction in plants. *Current Biology*, 7(9), R534–R537.

Micali, C.O., Neumann, U., Grunewald, D., Panstruga, R. & O'Connell, R. (2011) Biogenesis of a specialized plant-fungal interface during host cell internalization of *Golovinomyces orontii* haustoria. *Cellular Microbiology*, 13(2), 210–226.

Moran, D.T. & Rowley, J.C. (1987) Biological specimen preparation for correlative light and electron microscopy. In: Hayat, M.A. *Correlative microscopy in biology*. Cambridge: Academic Press, pp. 1–22.

Oehl, F., Laczko, E., Bogenrieder, A., Stahr, K., Bösch, R., van der Heijden, M. et al. (2010) Soil type and land use intensity determine the composition of arbuscular mycorrhizal fungal communities. *Soil Biology and Biochemistry*, 42(5), 724–738.

Peng, M., Hannam, C., Gu, H., Bi, Y.-M. & Rothstein, S.J. (2007) A mutation in *NLA*, which encodes a RING-type ubiquitin ligase, disrupts the adaptability of *Arabidopsis* to nitrogen limitation. *The Plant Journal*, 50(2), 320–337.

Peterhansel, C., Freialdenhoven, A., Kurth, J., Kolsch, R. & Schulze-Lefert, P. (1997) Interaction analyses of genes required for resistance responses to powdery mildew in barley reveal distinct pathways leading to leaf cell death. *The Plant Cell*, 9(8), 1397–1409.

Piffanelli, P., Zhou, F., Casais, C., Orme, J., Jarosch, B., Schaffrath, U. et al. (2002) The barley MLO modulator of defense and cell death is responsive to biotic and abiotic stress stimuli. *Plant Physiology*, 129(3), 1076–1085.

Reinstädler, A., Müller, J., Czembor, J.H., Piffanelli, P. & Panstruga, R. (2010) Novel induced *mlo* mutant alleles in combination with site-directed mutagenesis reveal functionally important domains in the heptahelical barley mlo protein. *BMC Plant Biology*, 10, 31.

Riveras, E., Alvarez, J.M., Vidal, E.A., Oses, C., Vega, A. & Gutiérrez, R.A. (2015) The calcium ion is a second messenger in the nitrate signaling pathway of Arabidopsis. *Plant Physiology*, 169(2), 1397–1404.

Sawaguchi, A., Ide, S., Goto, Y., Kawano, J.I., Oinuma, T. & Suganuma, T. (2001) A simple contrast enhancement by potassium permanganate oxidation for Lowicryl K4M ultrathin sections prepared by high pressure freezing/freeze substitution. *Journal of Microscopy*, 201(Pt 1), 77–83.

Schwarzbach, E. (1976) The pleiotropic effects of the *ml-o* gene and their implications in breeding. In: *Barley genetics III*. Karl Thiemig Verlag: München. pp. 440–445.

Veiga, R.S.L., Faccio, A., Genre, A., Pieterse, C.M.J., Bonfante, P. & van der Heijden, M.G.A. (2013) Arbuscular mycorrhizal fungi reduce growth and infect roots of the non-host plant *Arabidopsis thaliana*. *Plant, Cell & Environment*, 36(11), 1926–1937.

Wang, F., Wu, W., Wang, D., Yang, W., Sun, J., Liu, D. et al. (2016) Characterization and genetic analysis of a novel light-dependent lesion mimic mutant, *lm3*, showing adult-plant resistance to powdery mildew in common wheat. *PLoS One*, 11(5), e0155358.

Wang, J., Ye, B., Yin, J., Yuan, C., Zhou, X., Li, W. et al. (2015) Characterization and fine mapping of a light-dependent *leaf lesion mimic mutant 1* in rice. *Plant Physiology and Biochemistry*, 97, 44–51.

Wang, X., Feng, C., Tian, L., Hou, C., Tian, W., Hu, B. et al. (2021) A transceptor-channel complex couples nitrate sensing to calcium signaling in *Arabidopsis*. *Molecular Plant*, 14(5), 774–786.

Wen, B., Xiao, W., Mu, Q., Li, D., Chen, X., Wu, H. et al. (2020) How does nitrate regulate plant senescence? *Plant Physiology and Biochemistry*, 157, 60–69.

Wolter, M., Hollricher, K., Salamini, F. & Schulze-Lefert, P. (1993) The mlo resistance alleles to powdery mildew infection in barley trigger a developmentally controlled defence mimic phenotype. *Molecular and General Genetics MGG*, 239(1–2), 122–128.

Yuchun, R.A.O., Ran, J.I.A.O., Sheng, W.A.N.G., Xianmei, W.U., Hanfei, Y.E., Chenyang, P.A.N. et al. (2021) *SPL36* encodes a receptor-like protein kinase that regulates programmed cell death and defense responses in rice. *Rice*, 14(1), 34.

Zhang, X., Tian, B., Fang, Y., Tong, T., Zheng, J. & Xue, D. (2019) Proteome analysis and phenotypic characterization of the lesion mimic mutant *bspl* in barley. *Plant Growth Regulation*, 87(2), 329–339.

SUPPORTING INFORMATION

Additional supporting information can be found online in the Supporting Information section at the end of this article.

How to cite this article: Freh, M., Reinstädler, A., Neumann, K. D., Neumann, U. & Panstruga, R. (2024) The development of pleiotropic phenotypes in powdery mildew-resistant barley and *Arabidopsis thaliana mlo* mutants is linked to nitrogen availability. *Plant, Cell & Environment*, 47, 2360–2374. https://doi.org/10.1111/pce.14884